8-7-2016

Silver Photo-Diffusion and Photo-Induced Macroscopic Surface Deformation of Ge33S67/Ag/Si Substrate

M. Ailavajhala
Boise State University

M. Mitkova
Boise State University

Silver photo-diffusion and photo-induced macroscopic surface deformation of $Ge_{33}S_{67}$/Ag/Si substrate

Y. Sakaguchi,[1,a)] H. Asaoka,[2] Y. Uozumi,[2] K. Kondo,[2] D. Yamazaki,[2] K. Soyama,[2] M. Ailavajhala,[3] and M. Mitkova[3]
[1]*Neutron Science and Technology Center, Comprehensive Research Organization for Science and Society (CROSS), Tokai 319-1106, Japan*
[2]*Japan Atomic Energy Agency (JAEA), Tokai 319-1195, Japan*
[3]*Department of Electrical and Computer Engineering, Boise State University, 1910 University Dr. Boise, Idaho 83725-2075, USA*

(Received 1 June 2016; accepted 9 July 2016; published online 2 August 2016; corrected 11 August 2016)

Ge-chalcogenide films show various photo-induced changes, and silver photo-diffusion is one of them which attracts lots of interest. In this paper, we report how silver and Ge-chalcogenide layers in $Ge_{33}S_{67}$/Ag/Si substrate stacks change under light exposure in the depth by measuring time-resolved neutron reflectivity. It was found from the measurement that Ag ions diffuse all over the matrix $Ge_{33}S_{67}$ layer once Ag dissolves into the layer. We also found that the surface was macroscopically deformed by the extended light exposure. Its structural origin was investigated by a scanning electron microscopy. *Published by AIP Publishing.* [http://dx.doi.org/10.1063/1.4959207]

I. INTRODUCTION

Amorphous chalcogenides exhibit various structural changes caused by light illumination. The changes are initiated by the photo-excitation of lone-pair electrons to the anti-bonding states, and the structural flexibility of the amorphous materials allows them to change to metastable structure of the materials.[1] Silver photo-diffusion is one of the photo-induced phenomena and attracted many researchers since its discovery in 1966.[2,3] To realize the movement of ions from electron-excitation, there should be a delicate mechanism, in which ions, electrons, and phonons (network structure of amorphous materials) are closely related to each other. This effect has diverse applications such as photo-resist,[4] the fabrication of relief images in optical elements,[5] and non-volatile memory devices.[6] From both fundamental research and application points of view, it is important to know how silver photo-diffusion takes place. According to several studies using Rutherford backscattering (RBS), the photo-diffusion is unique to show a step-like profile of silver concentration in contrast to a usual diffusion in which the concentration gradually decreases as a function of distance from the silver layer.[7–9] Although RBS is a powerful technique to clarify concentration profiles of constitutional elements, *in situ* studies under light exposure were difficult because silver diffusion occurs also by a strong He^+ ion beam used for time-resolved measurement to get enough statistics in a short time.[8] Therefore, in the previous studies, several films with a different light exposure time have been prepared, and *ex situ* RBS studies were performed using weak He^+ ion beam. From the measurement, precise depth profiles as a function of exposure time have been obtained.[9,10] Due to the high sensitivity of the Ag photo-diffusion effect, it is desirable to perform *in situ* measurements using a proper probe beam which does not affect it. X-ray beam can be a good probe, but it can also induce silver diffusion when it is strong.[11] Recently, we focused our interest on neutron beam, which is not supposed to induce silver diffusion, and performed neutron reflectivity measurements of Ag/Ge-chalcogenide films.[12–15] From the measurements, time variation of the thicknesses of silver and reaction layers was clarified, and it was found that silver diffusion kinetics markedly depends on Ge compositions and the direction of light illumination (from Ag-side or Ge-chalcogenide-side). In this paper, we report the results of neutron reflectivity measurements of $Ge_{33}S_{67}$ 1500 Å/Ag 500 Å/Si substrate and $Ge_{33}S_{67}$ 2000 Å/Ag 500 Å/Si substrate stacks and to show how silver ions diffuse into $Ge_{33}S_{67}$ films, depending on the thickness of chalcogenide layer. In addition, through the measurements, we found that macroscopic pattern was formed by extended light exposure. In order to clarify the surface morphology and the spatial distribution of elements of interest, the films with the stacks have been investigated by scanning electron microscope equipped with energy dispersive X-ray spectroscopy (SEM-EDX). The structural origin of the macroscopic patterns is discussed based on the experimental results.

II. EXPERIMENTAL

X-ray/neutron reflectivity is one of the applications of optics[16] and is theoretically obtained by giving the scattering length density (SLD), the thickness, the roughness, and the modulus of the wave vector transfer Q, using Parratt's recursive method or Abeles matrix method.[17–19] The SLD is given by $\sum_i n_i(z)b_i(z)$, where n_i is the number density of the i-th nucleus at the distance of z from the interface and b_i is the scattering length of the nucleus. We assume a model of SLD profile as a function of depth, and the model is verified by a fit of the calculated reflectivity to the measured one. In addition, there are model-free analytical techniques, and Fourier transformation is one of the useful techniques to reveal basic

a)Electronic mail: y_sakaguchi@cross.or.jp

multi-layer structure of the films in terms of the number of layers and the thicknesses of the layers.[20,21]

The neutron reflectivity measurements were carried out on BL17 (*SHARAKU*)[22] at the Materials and Life Science Experimental Facility (MLF) of the Japan Proton Accelerator Research Complex (J-PARC). At the MLF, intense pulsed neutrons are generated through nuclear spallation reactions between a high-energy proton beam and the liquid-Hg neutron source target with a repetition rate of 25 Hz. The neutron flux is proportional to the power of the incident proton beam which was 300 kW in the present experiment. White light from a 300 W xenon lamp (MAX-303, ASAHI Spectra, Co., Ltd.) was used as an excitation light source, and the exposure of the sample was under computer-control. Neutron reflectivity, R, was obtained by $R = I/I_0$, where I is the intensity of the reflected beam and I_0 is the intensity of the incident beam as a function of neutron time-of-flight (TOF), t_{TOF}. I_0 was obtained by measuring the intensity of the direct beam without sample. The TOF was converted to Q, using the relationships: $\lambda = ht_{TOF}/mL$, where λ is the neutron wavelength, h is Planck's constant, m is the mass of a neutron, L is the length between the neutron source and the detector, and $Q = 4\pi \sin\theta/\lambda$ where $\theta = \theta_i$ (incident angle) $= \theta_f$ (scattering angle). Before light exposure, TOF spectra at two different angles, 0.4° and 0.8°, were measured, and these were combined to give a static single spectrum over a wide Q range. During light exposure, the sample was fixed at one angle, 0.4°, and the time evolution of the transient TOF spectrum was measured while exposing the sample to light from the xenon lamp. In the measurement, the slits were set to be $\Delta\theta/\theta = 5\%$. The details of the experimental procedure are shown in Ref. 14. At the MLF, neutron data are acquired using an event recording system in which every detected neutron is tagged with neutron pulse number, time taken from a facility-wide standard clock, and TOF. From the full recorded data set, arbitrarily time sliced TOF spectra were obtained using the data reduction system of the facility. The obtained neutron reflectivity profiles were fitted using the Motofit package.[23]

X-ray diffraction was measured by X-ray diffractometer (Rigaku Ultima III) with Cu K_α radiation. The measurement was performed by out-of-plane configuration. The surface of the films after the light exposure was observed by SEM (Zeiss SIGMA) equipped with EDX (Oxford Instruments X-Max 80 mm^2) at the acceleration voltage 15 kV. The samples were prepared using thermal evaporation applying a Cressington 308R coating system at 10^{-6} mbar vacuum. The thicknesses of the films were estimated using the output from a quartz crystal microbalance.

III. RESULTS AND DISCUSSION

A. Silver photo-diffusion kinetics in the depth direction probed by neutron reflectivity

1. Time-resolved neutron reflectivity

We measured time-resolved neutron reflectivity for two samples: $Ge_{33}S_{67}$ 1500 Å/Ag 500 Å/Si substrate and $Ge_{33}S_{67}$2000 Å/Ag 500 Å/Si substrate stacks. The results of the former sample have already been reported.[15] In this paper, we display the results of the latter one and discuss the silver diffusion kinetics based on the time variation of the parameters obtained from the results of both the samples.

Fig. 1 shows time evolution of neutron reflectivity profiles of $Ge_{33}S_{67}$ 2000 Å/Ag 500 Å/Si substrate stack during light exposure. The red curves show the calculated reflectivities obtained from model fittings. Before the light exposure, there are two types of oscillations with different intervals; 0.005 and 0.015 $Å^{-1}$, which represent the thickness of $Ge_{33}S_{67}$ and silver, respectively. In fact, the calculated neutron reflectivity profile, in which $Ge_{33}S_{67}$/Ag two layers are assumed, is well fitted to the experimental curve as shown in the figure. This means that the sample was intact without silver diffusion before the light exposure. After starting light exposure, the oscillation with the interval of 0.015 $Å^{-1}$ became unclear in the time from 2–4 to 6–8 min. This is attributed to the dissolution of silver into $Ge_{33}S_{67}$ layer. As for the amplitude of the oscillation with the interval of 0.005 $Å^{-1}$, it fluctuated; it became larger in the time from 2–4 to 12–14 min, first, and then, smaller in the time from 12–14 to 14–16 min, and lager again in the time from 14–16 to 24–26 min. The changes roughly indicate the changes in the thicker matrix chalcogenide layer. It should be noted that

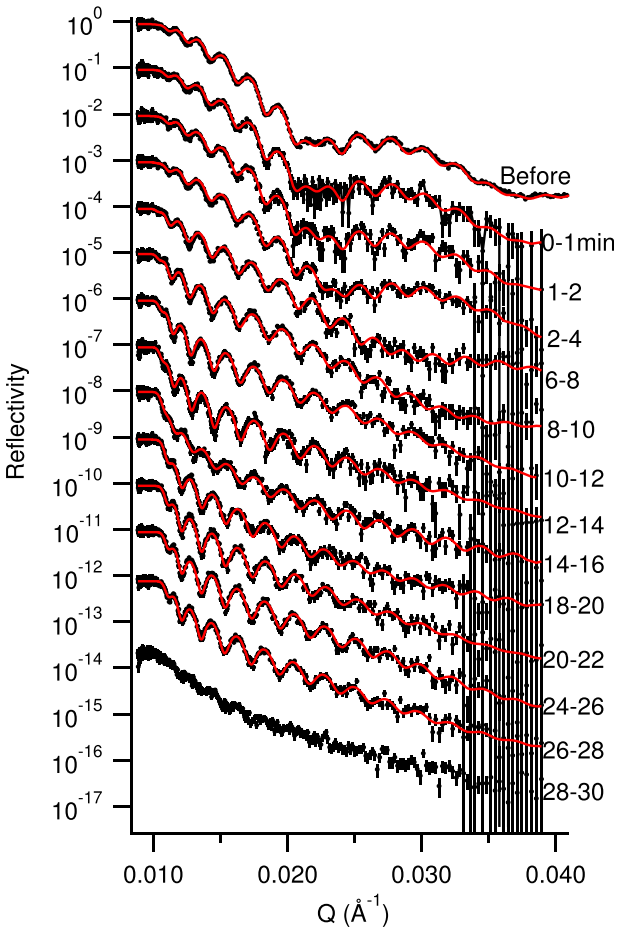

FIG. 1. Time evolution of neutron reflectivity profiles of $Ge_{33}S_{67}$ 2000 Å/Ag 500 Å/Si substrate stack during light exposure and the calculated curves by model fitting. The height of the vertical line on the experimental data indicates the error bar.

the oscillation was clearly preserved even after the silver photo-diffusion, which means that the layer is uniform in the depth direction. At 28–30 min, the neutron reflectivity rapidly changed with almost no oscillation and total reflection cannot be observed. The loss of the total reflection region could indicate that the surface has large roughness, which does not provide specular reflection. In fact, there was a visible change with macroscopic roughness on the surface as shown in Fig. 2. These features are very similar to the results of neutron reflectivity of $Ge_{33}S_{67}$ 1500 Å/Ag 500 Å/Si substrate[15] and $Ge_{40}Se_{60}$ 1500 Å/Ag 500 Å/Si substrate.[14]

In order to see the time evolutional change from different aspects, the integrated neutron intensities through whole TOF in 1 s are plotted as a function of light exposure time in Fig. 3. For both $Ge_{33}S_{67}$ 1500 Å/Ag 500 Å/Si substrate and $Ge_{33}S_{67}$ 2000 Å/Ag 500 Å/Si substrate stacks, the intensity started to decrease at the moment of light-on. Roughly speaking, this decrease could be related to the silver dissolution. For $Ge_{33}S_{67}$ 1500 Å/Ag 500 Å/Si, the intensity rapidly decreased in the first 1 min and it gradually decreased after the rapid decrease. At approximately 30 min, rapid decrease started again, and the intensity saturated at very weak level, which is 1/10 of the initial one. For $Ge_{33}S_{67}$ 2000 Å/Ag 500 Å/Si, the intensity monotonously decreased after the light-on, increased after 17 min light exposure, and then dropped at 27 min.

To clarify when the macroscopic visible roughness was produced, the neutron reflectivity in the total reflection region is plotted as a function of light exposure time as shown in Fig. 4. As shown in the figure, the neutron reflectivity in the total reflection region dropped at 30 min for $Ge_{33}S_{67}$ 1500 Å/Ag 500 Å/Si and 27 min for $Ge_{33}S_{67}$ 2000 Å/Ag 500 Å/Si, respectively. The decrease of the neutron reflectivity is rapid in $Ge_{33}S_{67}$ 2000 Å/Ag 500 Å/Si, while it is gentle in $Ge_{33}S_{67}$ 1500 Å/Ag 500 Å/Si. Summing up these results in Figs. 1–3, it was found that: (1) the macroscopic surface roughness started to be produced at 30 min for $Ge_{33}S_{67}$ 1500 Å/Ag 500 Å/Si, and at 27 min for $Ge_{33}S_{67}$ 2000 Å/Ag 500 Å/Si; (2) there could be two diffusion or reaction processes, 0–1 min and 1–30 min, for $Ge_{33}S_{67}$ 1500 Å/Ag 500 Å/Si; and (3) there could also be two diffusion or reaction processes, 0–17 min and 17–27 min, for $Ge_{33}S_{67}$ 1500 Å/Ag 500 Å/Si.

FIG. 2. Photograph of $Ge_{33}S_{67}$ 2000 Å/Ag 500 Å/Si substrate stack after 65 min light exposure. The sample size is about 30 mm × 30 mm, and the exposed area is 27 mm × 27 mm.

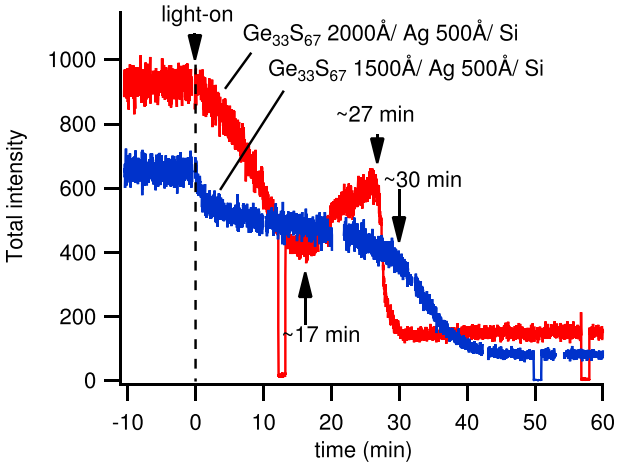

FIG. 3. Time variation of integrated reflected neutron intensities through whole TOF spectrum.

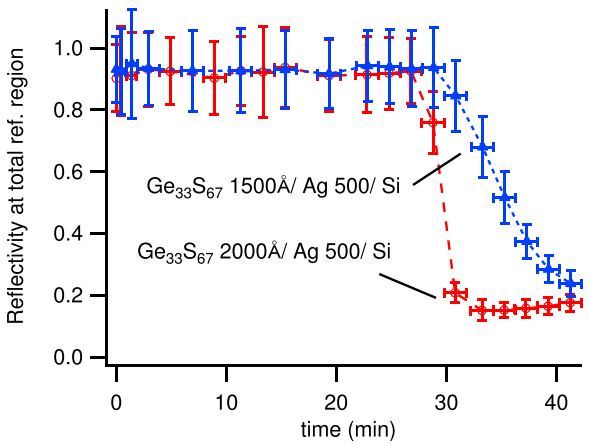

FIG. 4. Time variation of neutron reflectivity in the total reflection region.

To elucidate the silver diffusion process, it is important to know the time evolutional change in the basic stack structure, such as the number of layers and the thicknesses of the layers, and Fourier transformation is one of the useful model-free techniques to clarify such layer structure. Fig. 5 shows time evolution of Fourier transform of the neutron reflectivity of $Ge_{33}S_{67}$ 2000 Å/Ag 500 Å/Si. Before the light exposure, there are three peaks at 400, 2400, and 3000 Å, which indicate the thickness of the layer of Ag, $Ge_{33}S_{67}$, and the sum of these layers, respectively. This confirms that the multi-layer structure of $Ge_{33}S_{67}$ 2000 Å/Ag 500 Å/Si stack was preserved from the sample preparation and that silver diffusion did not occur before light exposure. The features of the peaks changed after light-on.

Fig. 6 shows the time variation of the peak positions in the Fourier transform in Fig. 5. In the figure, the result of $Ge_{33}S_{67}$ 1500 Å/Ag 500 Å/Si stack is also included for comparison. The first peak around 400 Å represents the Ag layer. This peak decreases after light exposure for both of the stacks. However, the peak of $Ge_{33}S_{67}$ 1500 Å/Ag 500 Å/Si

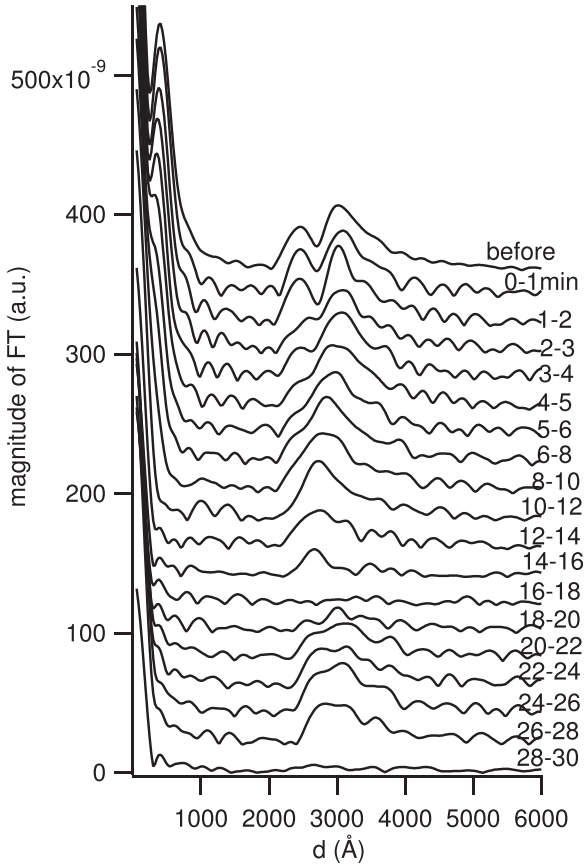

FIG. 5. Time evolution of Fourier transform of the neutron reflectivity of $Ge_{33}S_{67}$ 2000 Å/Ag 500 Å/Si.

stack seems to saturate approximately at 300 Å, while it seems to continue to decrease for $Ge_{33}S_{67}$ 2000 Å/Ag 500 Å/Si stack. The difference between 2nd and 3rd peaks could also indicate the presence of Ag layer indirectly, and the result seems to be consistent with that of the first peak. Since the measured Q-region was limited to 0.04 $Å^{-1}$ as a maximum in the present experiment, the observable minimum thickness was limited to about 300 Å.

To compensate this limit, a model fitting would be useful. However, it is important to establish a plausible model prior to performing the fitting. Especially, the transient reflectivity sliced with a short time period, such as 1 min, should be treated very carefully because the signal to noise ratio is poor in the Q-range from 0.02 to 0.04 $Å^{-1}$. In order to obtain reliable models for the transient data, we first fix a reliable model for the neutron reflectivity before light exposure, which was obtained from two time-of-flight spectra with different incident/scattering angles, and is supposed to have enough statistics. Actually, the obtained layer model is consistent with the designed layer structure in thermal evaporation, showing that the two layers are intact without silver diffusion. For the curve fitting to the transient data, the parameters were changed starting from those of the initial state. In addition, the results of Fourier transform in Figs. 5 and 6 were used to limit the thickness parameters in the model fitting to the transient data. Furthermore, the content of residual Ag layer in the stacks after light exposure was examined by X-ray diffraction measurement, as shown in Fig. 7. Obviously, there is Ag crystal in the $Ge_{33}S_{67}$ 1500 Å/Ag 500 Å/Si stack,[15] and the peak height is about 0.24 compared to that of the samples without light exposure. Considering the result, it is good to include a Ag layer in the layer model through the light exposure for $Ge_{33}S_{67}$ 1500 Å/Ag 500 Å/Si stack.[15] The result also supports our expectation on the 1st peak in Fig. 6 that the thickness of Ag layer was saturated approximately at 300 Å. For $Ge_{33}S_{67}$ 2000 Å/Ag 500 Å/Si stack, there is a small amount of Ag crystal and the peak height is about 0.03 compared to that of the samples without light exposure. In this case, we can assume that Ag layer is consumed almost in full by silver photo-diffusion.

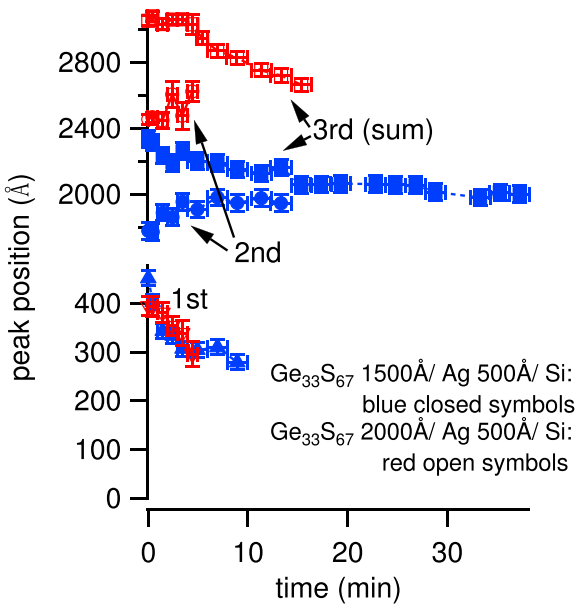

FIG. 6. Time variation of the peak position in the Fourier transform shown in Fig. 5.

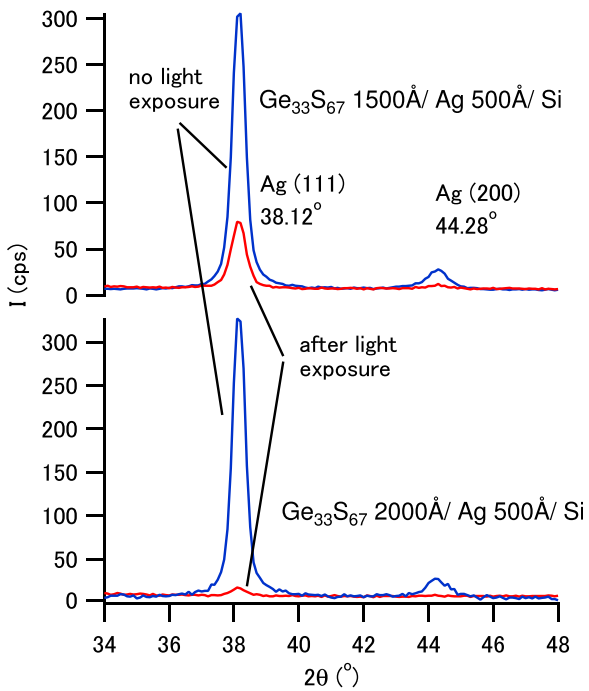

FIG. 7. X-ray diffraction of $Ge_{33}S_{67}$ 1500 Å/Ag 500 Å/Si and $Ge_{33}S_{67}$ 2000 Å/Ag 500 Å/Si stacks.[15]

The result also supports the expectation on the 1st peak in Fig. 6 that Ag layer is continuously becoming thinner.

Fig. 8 shows the time variation of the SLD profile, which is the result of the layer model obtained from the fitting to the neutron reflectivity curve in Fig. 1. As shown in Fig. 1, the calculated curves obtained from a model fitting are in good agreement with the experimental curves almost within the error bars. The SLD of Ag is 3.47×10^{-6} Å^{-2}, while the SLD of a-$Ge_{33}S_{67}$ is 1.95×10^{-6} Å^{-2}. Up to 16 min, the time variation of the SLD profile looks reasonable, showing that the Ag layer becomes thinner with light exposure time. It is noted that Ag does not diffuse exponentially but diffuses into the matrix amorphous chalcogenide (a-Ch) layer keeping a step-like distribution (uniform Ag distribution). This is consistent with the previous results of Rutherford backscattering.[7–9] After 16 min, fitting was not successful by only assuming the disappearance of Ag layer. Therefore, we assumed a less SLD region, suggesting formation of a vacancy, for the time after 18–20 min. This would be a trial fitting, but the presence of the vacant region could indicate a sort of a precursor of the formation of macroscopic roughness which appears after 27 min exposure time.

Fig. 9 shows time variations of thicknesses of the layers, the Ag layer and the matrix a-Ch layer, in $Ge_{33}S_{67}$ 1500 Å/Ag 500 Å/Si and $Ge_{33}S_{67}$ 2000 Å/Ag 500 Å/Si stacks, which were obtained from the fitting to the neutron reflectivity curves. For $Ge_{33}S_{67}$ 1500 Å/Ag 500 Å/Si, a Ag layer rapidly decreases in the first 1 min and then saturates around 150 Å. For $Ge_{33}S_{67}$ 2000 Å/Ag 500 Å/Si, a Ag layer decreases with exposure time and then almost vanishes around 16 min. On the other hand, the matrix a-Ch layer expands with time according to the introduction of Ag ions for both of the stacks.

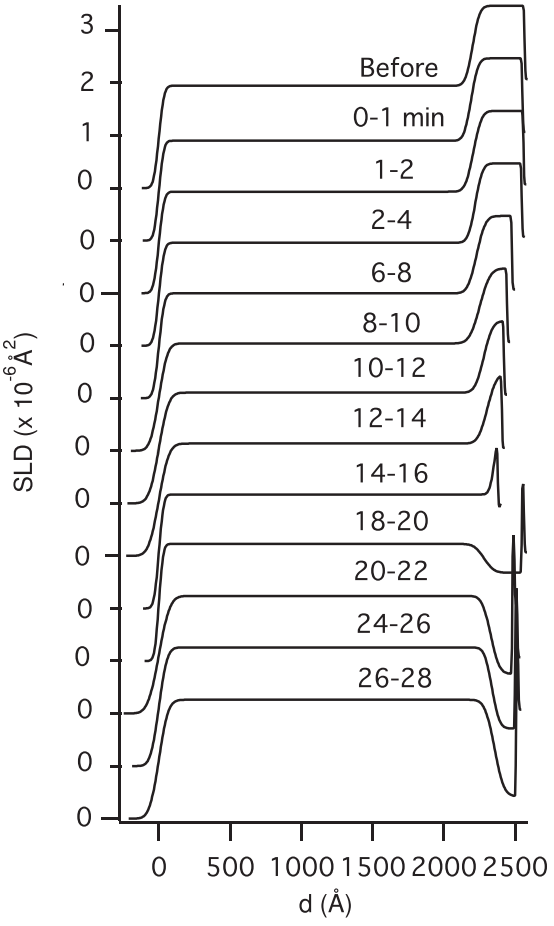

FIG. 8. Time variation of the SLD profile obtained from fitting to the neutron reflectivity curve in Fig. 1.

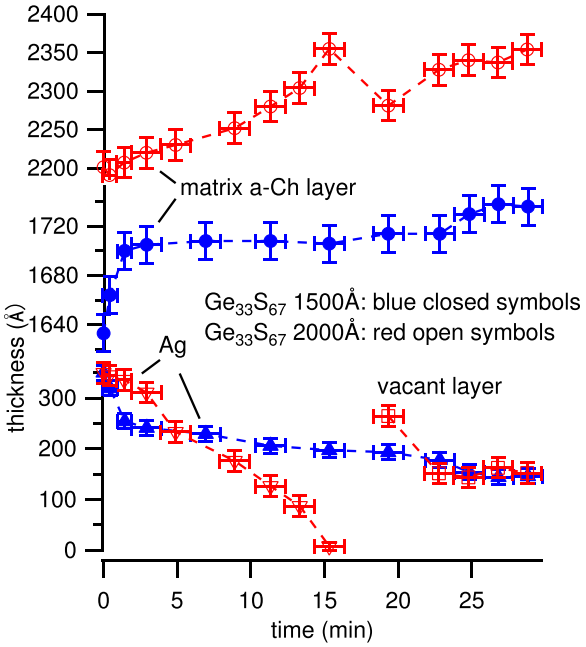

FIG. 9. Time variations of thicknesses of the layers (Ag layer and matrix amorphous chalcogenide (a-Ch) layer) in $Ge_{33}S_{67}$ 1500 Å/Ag 500 Å/Si and $Ge_{33}S_{67}$ 2000 Å/Ag 500 Å/Si stacks, which were obtained from the fitting to the neutron reflectivity curves.

Fig. 10 shows time variations of SLDs of the layers, the Ag layer and the matrix a-Ch layer, in $Ge_{33}S_{67}$ 1500 Å/Ag 500 Å/Si and $Ge_{33}S_{67}$ 2000 Å/Ag 500 Å/Si stacks. The SLD of the Ag layer should be constant. For $Ge_{33}S_{67}$ 2000 Å/Ag 500 Å/Si, the SLD of the matrix a-Ch layer increases with

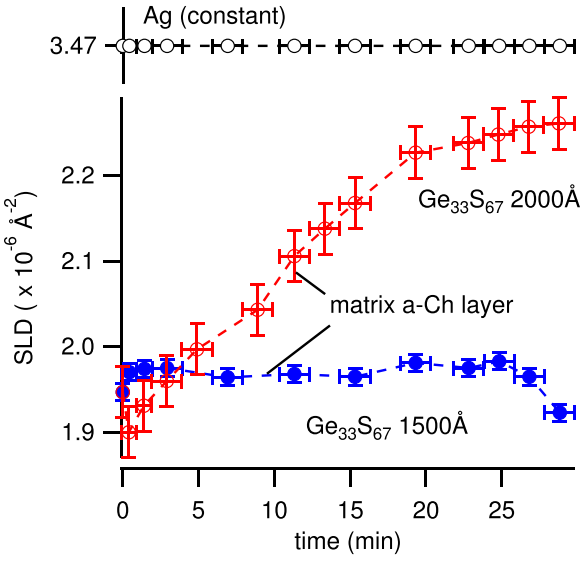

FIG. 10. Time variations of the SLDs of the layers, the Ag layer and the matrix a-Ch layer, in $Ge_{33}S_{67}$ 1500 Å/Ag 500 Å/Si and $Ge_{33}S_{67}$ 2000 Å/Ag 500 Å/Si stacks. The SLD of the Ag layer should be constant.

exposure time. This is reasonably explained by the increase of Ag ion concentration as a result of silver photo-diffusion. For $Ge_{33}S_{67}$ 1500 Å/Ag 500 Å/Si, the increase in the SLD of the matrix a-Ch layer is also observed in the first 1 min, suggesting the increase of Ag ion concentration.

2. Kinetics of silver photo-diffusion

Overall, silver diffusion in $Ge_{33}S_{67}$/Ag/Si can be described by two layers system; the matrix a-Ch layer and the Ag layer. This means that there is no "metastable Ag-rich reaction layer" between the Ag layer and the matrix a-Ch layer, which can act as an interface layer, and whose model was assumed to understand silver photo-diffusion in $Ag/Ge_{20}S_{80}/Si$.[12] These two models are illustrated in Fig. 11. The difference of the models is basically explained by the number of the potential barriers; Ag/Ag-rich reaction (metastable) layer/Ag-poor reaction layer has two potential barriers, while the matrix a-Ch layer/Ag has only one potential barrier. In the former case, the two barriers provide different reaction rates. The first barrier at the Ag layer/Ag-rich reaction layer interface may be lower and the reaction rate may be faster, while the second barrier at the Ag-rich reaction layer/Ag-poor reaction layer may be greater and the reaction rate may be slower. In the latter case, Ag ions are supposed to move almost freely in the matrix a-Ch layer once they get over the barrier at the matrix a-Ch layer/Ag interface.

This discrepancy may be explained by the difference of the light exposure side, as illustrated in Fig. 12. The transmission, T, was calculated from the relationship: $T = \exp(-\alpha x)$, where α is the absorption coefficient and x is the distance of the medium. The α of silver and a-$Ge_{33}S_{67}$ (GeS_2) was estimated from Refs. 24 and 25, respectively. In the present experiment, a white light of xenon lamp was used. In the figure, the transmission of the light with the wavelength of 397 nm, which has greater energy (3.12 eV) than the optical gap, 2.59 eV,[25] is shown. Supposing that the light is used to excite lone-pair electrons to anti-bonding states on chalcogen (S) atoms, the efficiency of the photo-excitation should be proportional to the transmission of light whose energy has greater than the optical gap, and "chalcogen atoms" should be exposed to the light. In essence, Ag diffusion is supposed to take place only at the two interfaces, Ag/Ag-doped layer and Ag-doped layer/a-Ch, which are exposed to the light. When the sample is exposed to the light from Ag layer side, the transmission has the highest value at Ag/a-Ch interface with a few percent among the whole chalcogen atoms in the layer. Therefore, we assume that dominant photo-induced effect occurs near the interface region, and a metastable Ag-rich reaction layer is formed as the first stage of the Ag diffusion process. Since the optical transmission decreases with increasing Ag content,[26] the effect of the light to the metastable Ag-rich reaction layer/a-Ch interface can be smaller, and thus, it would be reasonable to expect the slow diffusion which takes place at the interface. In the case when the sample is exposed to the light from chalcogenide side, both the whole chalcogenide bulk and matrix a-Ch/Ag interface are affected by the

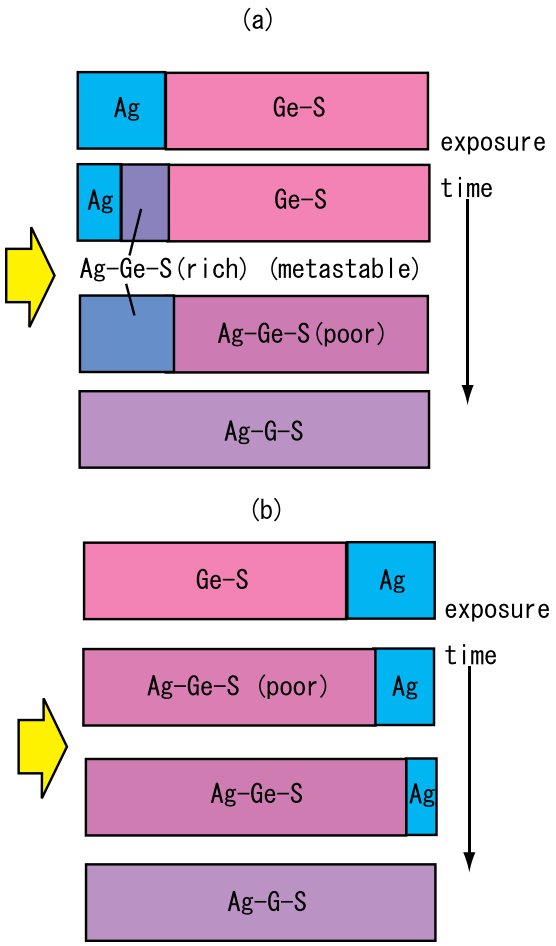

FIG. 11. Two models of silver photo-diffusion. (a) There is a metastable Ag-rich reaction layer. (b) Ag ions diffuse almost freely all over the matrix a-Ch layer without forming a metastable reaction layer once Ag dissolves into the layer. The sample is exposed to the light from left-hand side.

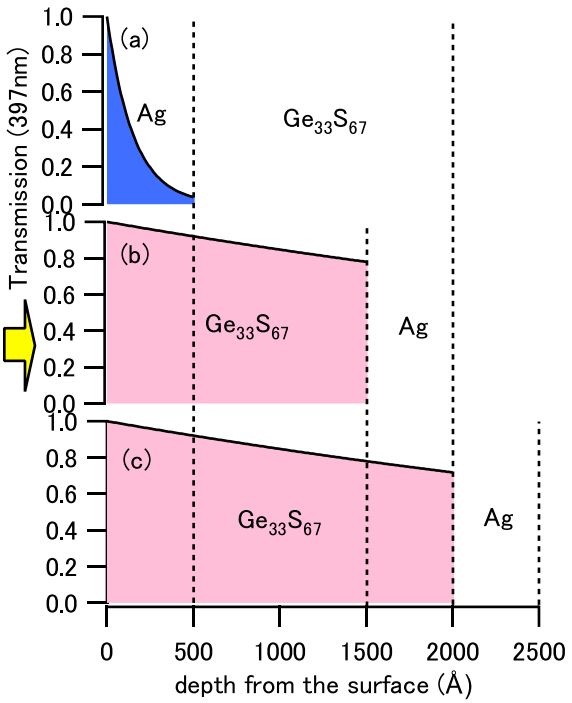

FIG. 12. Schematic illustration of the light exposure effect on (a) Ag 500 Å/$Ge_{33}S_{67}$ 1500 Å/Si, (b) $Ge_{33}S_{67}$ 1500 Å/Ag 500 Å/Si, and (c) $Ge_{33}S_{67}$ 2000 Å/Ag 500 Å/Si.

light. As the first step of silver photo-diffusion, the light should affect the a-Ch/Ag interface and Ag ions are supplied into a-Ch layer across the interface. After that, the light affects a-Ch/Ag-doped interface, but the front of the interface is supposed to proceed to the end of a-Ch layer, because the interface is always exposed to the light with enough intensity. As a result, Ag ions are supposed to move almost freely in the matrix a-Ch layer. The present result also demonstrated that amount of silver dissolution depends on the thickness of chalcogenide layer. Thicker chalcogenide layer supports more intensive dissolution of silver. This makes sense if we assume that negatively-charged defects are created on chalcogen (S) sites by the photo-excitation of lone-pair electrons, and that they trap positively-charged silver ions. This type of model is proposed by Kluge[27] and is known as the "intercalation model". In this case, the amount of silver dissolved in the chalcogenide layer depends on the amount of chalcogen atoms in it and, thus, the thickness of chalcogenide layer. Considering the silver photo-diffusion process from the light exposure, there would be a following scenario.[28–30] Undoubtedly, photo-excitation of lone-pair electrons in chalcogen atoms creates holes. Presumably, the holes can flow into Ag layer because of the energy levels at the junction and their mobility. As a result, the electrons are left on chalcogen sites, forming negatively-charged defects. In addition, there could be a counter flow of positively-charged Ag ions from Ag layer to a-Ch layer, which is the opposite direction of the flow of positively-charged holes from a-Ch layer to Ag layer. According to the model, the amount of chalcogen atoms limits the amount of Ag ions from Ag layer, and the present result is consistent with the previous models. Supposing that all Ag ions in the Ag layer diffuse into the $Ge_{33}S_{67}$ layer in the $Ge_{33}S_{67}$ 2000 Å/Ag 500 Å/Si stack before light exposure, which would actually be $Ge_{33}S_{67}$ 2200 Å/Ag 350 Å/Si according to the neutron reflectivity result, and a homogeneous reaction layer is produced, the reaction compound is estimated to be $Ag_{0.20}Ge_{0.27}S_{0.53}$. The actual Ag content is supposed to be a little bit smaller because a small amount of Ag did not photo-diffuse as shown in Fig. 7. Elliott[29] pointed out that the composition of the silver photo-doped region of a-$GeSe_2$ at saturation was $Ag_{0.28}Ge_{0.24}Se_{0.48}$ and that the composition of the silver photo-doped region obtained from Ag/a-$Ge_{0.29}S_{0.71}$ was $Ag_{0.23}Ge_{0.23}S_{0.54}$. Kawaguchi and Maruno[31] have shown that the total amount of photo-doped Ag into Ge_xS_{100-x} for $x = 30$ and $x = 34$ was quite similar. Roughly speaking, the present estimated value is comparable to these previously reported data.

Also, the a-Ch thickness dependence on the silver diffusion reaction rate is noted. As shown in Fig. 9, for $Ge_{33}S_{67}$ 1500 Å/Ag 500 Å/Si stack, Ag thickness rapidly decreases in the first 1 min and decreases slowly after the time. So far, it has been pointed out that the silver diffusion kinetics often follow parabolic kinetics, $\Delta X = (2kt)^{1/2}$,[29,32] where ΔX is a measure of the extent of the reaction, k is a constant, and t is time. However, it was difficult to fit to a parabolic form for this time variation of Ag thickness. The process in the first 1 min seems to be different from that in the time after the first 1 min. In the first 1 min, Ag dissolution occurs quickly probably due to enough vacancy to accept Ag ions in the chalcogenide layer, while the vacancies are supposed to be saturated after the first 1 min, resulting in the slow variation. On the other hand, for $Ge_{33}S_{67}$ 2000 Å, the Ag thickness almost linearly decreases with time by its disappearance with slower reaction rate, compared to that in the first 1 min for $Ge_{33}S_{67}$ 1500 Å. It is difficult to understand why such difference in the reaction rate appears between $Ge_{33}S_{67}$ 1500 Å and $Ge_{33}S_{67}$ 2000 Å. One of the reasons could be the light intensity at the interface as shown in Fig. 12. The light intensity at the interface depends on the thickness of chalcogenide layer; the thicker, the weaker, and the thinner, the stronger. Actually, Goldschmidt and Rudman have shown that the reaction rate, k, is basically followed by the relationship; $k \propto \alpha I_0 \exp[-\alpha d]$, where I_0 is the light intensity of the chalcogenide surface and d is the thickness of the chalcogenide layer, from the experimental result for a-As_2S_3/Ag.[33] Tanaka[28] has also shown the chalcogenide layer dependence on the reaction rate. These results are consistent with the present one, indicating that the reaction rate is slower for the thicker chalcogenide layer. However, there could be a factor to determine the time dependence of Ag thickness in addition to the transmission of a-Ch at the interface. It should be noted that α in matrix a-Ch layer changes once the silver diffusion starts. According to the previous work by Kawaguchi *et al.*,[26] the transmission of Ag-doped Ge-chalcogenide is smaller than that of non-doped Ge-chalcogenide. Therefore, the transmission at the interface decreases as the silver diffusion progresses. In other words, the reaction rate becomes slower as the Ag content increases in the matrix a-Ch layer. Probably, the successive increase of Ag content makes the situation more complicated and is supposed to result in the almost linear time dependence in $Ge_{33}S_{67}$ 2000 Å/Ag 500 Å/Si stack.

We finally remark on the discrepancy between the present result and the previous Ag diffusion model, stating the progression of the diffusion front.[9,10] Between the experiments, there are several differences in the experimental conditions, such as compositional elements (germanium sulfide or arsenic sulfide), chalcogenide layer thickness (200 nm or 960 nm), light exposure condition (*in situ* or *ex situ*), and used technique (neutron reflectivity or Rutherford backscattering). As seen in above discussion, the process of Ag diffusion markedly depends on Ge compositions and light illumination side, and those experimental results indicate that the difference in the experimental condition should carefully be treated. Probably, the problem can only be solved by performing experiments using the two techniques for the same sample and the same light exposure condition.

B. Structural origin of the surface with macroscopic roughness

It is also interesting to know what the final product with macroscopic surface roughness is made of. In fact, in our previous observations,[13,15] we assumed the appearance of a new photo-induced reaction stage such as Ag deposition[26] and phase separation. For this purpose, we first observed the surface using an optical microscope. Fig. 13 is the image of $Ge_{33}S_{67}$ 2000 Å/Ag 500 Å/Si observed by an optical

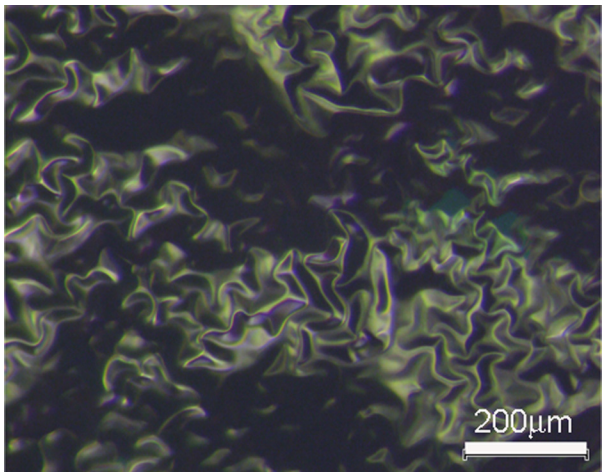

FIG. 13. Image of $Ge_{33}S_{67}$ 2000 Å/Ag 500 Å/Si substrate stack after light exposure observed by an optical microscope.

microscope. The image of $Ge_{33}S_{67}$ 1500 Å/Ag 500 Å/Si is very similar, which has already been reported.[15] It seems that there are mountains and valleys, which correspond to the grey and black portions, respectively. From such image, we could imagine that there are topographical height variations on the surface, or, there are two different phases with different colors, suggesting phase separation. Considering that Ag-rich $(Ge_{0.3}S_{0.7})_{100-x}$ Ag_x films exhibit silver deposition by light illumination,[34] photo-induced silver deposition is one of the candidate to explain the occurrence of such phase separation. However, the XRD studies did not demonstrate availability of pure Ag in the case of 2000 Å thick chalcogenide films and so do not support occurrence of phase separation. Besides, as far as we changed the height of the objective lens, and adjusted focus on several portions, we found that the focusing point depended on the portion in the image and the idea about surface roughness formation seems to be quite plausible.

Fig. 14 is the SEM image of $Ge_{33}S_{67}$ 1500 Å/Ag 500 Å/Si. Before observing the image, some portions were peeled off and both the remaining film part (the upper half, and the lower and right quarter) and the peeled-off part (the lower and left quarter) are observed in the image. Since the image

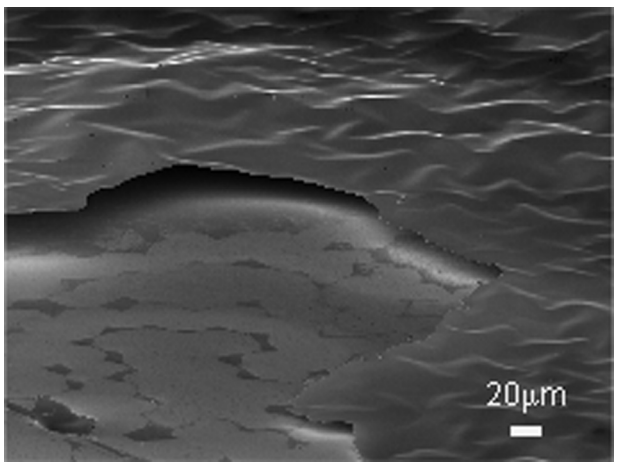

FIG. 14. SEM image of $Ge_{33}S_{67}$ 1500 Å/Ag 500 Å/Si substrate stack.

was taken by tilting the sample (70°), it looks like three-dimensional image, including height information. Obviously, the remaining film has wavy-like height variations. Also, the smooth color variation indicates that the remaining film is made of homogeneous sheet. In the peeled-off part, there are rounds with different sizes and they overlap with each other. Since thin Ag layer should still stays on the Si substrate in the stack as the XRD result in Fig. 7 suggests, these rounds could indicate the Ag layer. From these results, it can be concluded that the final product with macroscopic pattern is homogeneous substance with topographical height variations, not a mixture of two phases associated with phase separation. Interestingly, there is a gap between the film and the substrate. This may also indicate that there are large movements of the film along the height direction, and there could be some processes to reach this stage. In Fig. 10, we assumed a layer with less SLD value, which could have vacancies in the layer. Probably, such change would be a precursor of the movement along the height direction, resulting in the gap and peeling off from the substrate.

Fig. 15 shows the SEM image (a) and EDX element maps (b: Si, c: Ge, d: S and e: Ag) of $Ge_{33}S_{67}$ 1500 Å/Ag 500 Å/Si stack after extended light exposure. As shown in the maps, the film with wavy-like patterns (the upper half in the image) is composed of Ge, S, and Ag. This result strongly supports the idea that it is homogenous sheet and that phase separation did not occur. In the peeled-off portion (the lower half in the image), there are no distributions of Ge and S, but, weak Ag distribution can be detected on the round portions. This means that there is a small amount of

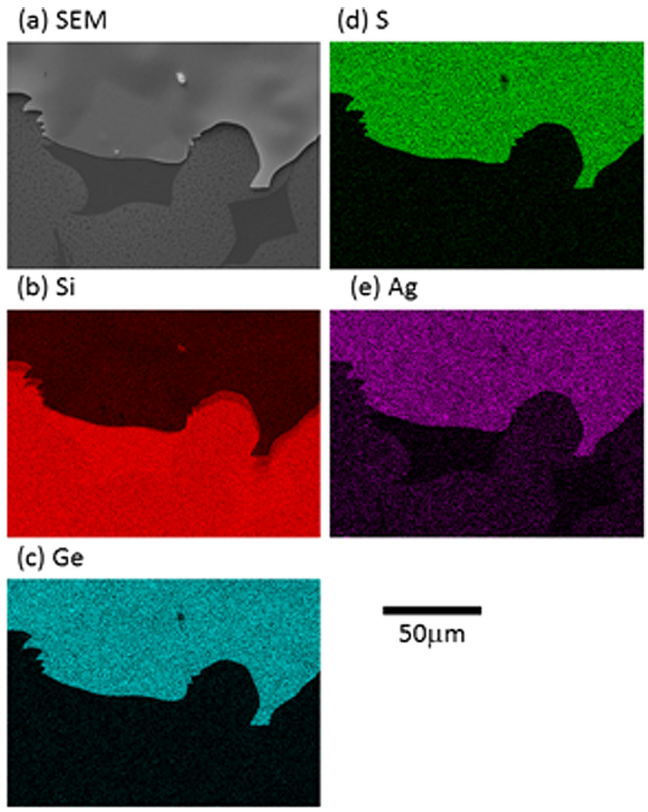

FIG. 15. SEM image (a) and EDX element map maps ((b): Si, (c): Ge, (d): S, and (e): Ag) of $Ge_{33}S_{67}$ 1500 Å/Ag 500 Å/Si stack.

silver on the round portions. This is consistent with the XRD result in Fig. 7, suggesting that a part of silver layer was left on the substrate, stopping silver dissolution somewhere in $Ge_{33}S_{67}$ 1500 Å/Ag 500 Å/Si stack. It may be noted that Ag film did not uniformly cover the Si substrate and patched round patterns were formed for Ag distributions. This could indicate that silver diffusion did not occur uniformly on the plane. Since the neutron reflectivity result only tells us the SLD profile along the depth direction, this information is very important to understand the silver photo-diffusion phenomenon together with the neutron reflectivity result.

It is also noted that the film "moved" somehow in a macroscopic scale only by light illumination which causes the electron excitation in the film. To realize such change, the film must be "liquid" or have liquid-like viscosity for a while (for instance, during light exposure), and all ions (Ag, Ge and S) become mobile, and then, it must be quenched to be amorphous state (for instance, after stopping light exposure) as we observed the solid surface by an optical microscope and SEM. As is well-known, liquid surface or liquid films can be structured with specific shapes due to the effect of a surface energy (surface tension), which originates from a termination or boundary of the phase. The shape depends on the liquid, the substrate, and several conditions such as the thickness, the temperature, and so on. The principles and various examples are summarized in Ref. 35. Therefore, we infer that the observed macroscopic patterns were formed through two processes: (1) softening of the film to liquid-like state and (2) changing the shape of the surface.

As for the first process, softening of the film, the possibility would be plausible because athermal photo-induced fluidity was previously reported for chalcogenide glasses (amorphous As_2S_3),[36] in which the excitation of lone-pair electrons by intensive subgap light illumination may play a crucial role. Also for amorphous Ge-chalcogenide films, the excitation of lone-pair electrons causes structural change.[37] In the present study, a white light of xenon lamp is used and the bandgap itself is supposed to change by the addition of Ag in the Ag-Ge-S system.[26] Therefore, we assume that the photo-induced fluidity occurred by the change of the bandgap and the supply of the subgap illumination from the white light of the xenon lamp. According to the SEM-EDX measurement for $Ge_{33}S_{67}$ 2000 Å/Ag 500 Å/Si stack, the compositional ratio of Ag-Ge-S film was $Ag_{0.215}(Ge_{0.38}S_{0.62})_{0.785}$. Supposing that the silver was fully diffused into the chalcogenide matrix in the stack, the result suggests that about 20% of Ag was diffused in the layer. This is compared to the compositional ratio estimated from the original $Ge_{33}S_{67}$ 2000 Å/Ag 500 Å/Si stack, $Ag_{0.20}Ge_{0.27}S_{0.53}$, as we discussed above. According to Aniya and Shinkawa,[38] the Ge_xS_{1-x} system can incorporate the largest amount of Ag at $x = 33$ (GeS_2) when the network structure of Ge-S changes from 2-dimensional to 3-dimensional and the fragility shows a minimum. Presumably, such anomaly in the system can be related to the realization of photo-induced fluidity. Although the present study indirectly indicates the possibility of photo-induced fluidity in the system, a direct observation is required to make sure our expectation.

As for the second process and how such specific wavy-like patterns were formed, previous reports with similar patterns can be referred. As far as we know, similar patterns are observed on thin films when they are prepared in specific conditions. For instance, similar wavy-like (wrinkle) patterns were observed in the process of diamond-like carbon film preparation by plasma deposition.[39,40] Such pattern formation was treated as a failure in the film preparation. The patterns were formed due to the internal compressive stress caused by unpaired dangling bonds on hydrogen atoms in the deposition gas mixture. In general, such wrinkle pattern can be formed when films have compressive strain due to some reasons, such as a mismatch in the thermal expansion coefficient and a change in the volume by reactions. Recently, such pattern formation is studied to utilize in producing self-organized microstructure. For instance, a photo-induced wrinkled microstructure formation with long-range-order in thin oxide films is reported.[41] Furthermore, similar wrinkle patterns were observed in liquid sulfur when a pulsed laser with the wavelength of 355 nm illuminates liquid sulfur with a thickness of 2 mm.[42] In this case, a high-viscous layer can be created on the surface by photo-induced polymerization in the system.[43] The appearance of the layer may cause new interaction with underneath low-viscous liquid composed of S_8 rings at the interface which could result in such wrinkle patterns formation. Those examples indicate that the present wrinkle patterns should be formed by specific conditions at the interface.

IV. CONCLUSIONS

We measured time-resolved neutron reflectivity of $Ge_{33}S_{67}$/Ag/Si stacks and showed how silver diffuses into Ge-chalcogenide layer by the light exposure. In contrast to Ag/$Ge_{20}S_{80}$/Si stacks, there is no metastable interface layer between matrix Ge-chalcogenide layer and Ag layer, and Ag ions diffuse almost freely all over the matrix Ge-chalcogenide layer once silver dissolves into the matrix Ge-chalcogenide layer. It was also found that thicker Ge-chalcogenide layer can absorb more silver, and that silver diffusion cannot be completed when the thickness of Ge-chalcogenide layer is not enough. There was a difference in the reaction rate between $Ge_{33}S_{67}$ 1500 Å/Ag 500 Å/Si stack and $Ge_{33}S_{67}$ 2000 Å/Ag 500 Å/Si stack. This could be due to the difference of the absorbed Ag content, but the details should be examined by further studies. In addition to the silver photo-diffusion kinetics, we found that a macroscopic roughness appeared on the samples by the extended light exposure approximately over 30 min. The SEM observation revealed that there are wavy-like height variations on the surface, and the surface is made of the homogeneous Ag-Ge-S film. Formation of such patterns indicates that the surface film becomes soft, like liquid. It is interesting to know why and how such softening could be realized. Furthermore, the formation of the macroscopic patterns stimulates our interest on spontaneous self-organization.

ACKNOWLEDGMENTS

This work was supported by JSPS Grant-in-Aid for Scientific Research (C), Grant No. 25400435. The neutron reflectivity measurements were performed on BL17 (*SHARAKU*) in J-PARC MLF under Project No. 2013B0159. We would like to thank N. Miyata, K. Akutsu, T. Ito, and S.

Kasai (CROSS) for technical support on the neutron reflectivity instrument, and R. Maruyama (JAEA) for technical support on X-ray diffraction measurements. This work has also been funded by the Defense Threat Reduction Agency under Grant No. HDTRA1-11-1-0055.

[1]*Photo-Induced Metastability in Amorphous Semiconductors*, edited by A. V. Kolobov (Wiley-VCH, Weinheim, 2003).
[2]M. T. Kostyshin, E. V. Mikhailovskaya, and P. F. Romanenko, Sov. Phys. (Solid State) **8**, 451 (1966).
[3]A. V. Kolobov and S. R. Elliott, Adv. Phys. **40**, 625 (1991).
[4]A. Yoshikawa, O. Ochi, H. Nagai, and Y. Mizushima, Appl. Phys. Lett. **29**, 677 (1976).
[5]J. Hajto, P. J. S. Ewen, R. E. Belford, and A. E. Owen, Thin Solid Films **200**, 229 (1991).
[6]M. Mitkova and M. N. Kozicki, J. Non-Cryst. Solids **299–302**, 1023 (2002).
[7]Y. Yamamoto, T. Itoh, Y. Hirose, and H. Hirose, J. Appl. Phys. **47**, 3603 (1976).
[8]J. Rennie, S. R. Elliott, and C. Jeynes, Appl. Phys. Lett. **48**, 1430 (1986).
[9]T. Wagner, V. Perina, M. Vlcek, M. Frumer, E. Rauhala, J. Saarilahti, and P. J. S. Ewen, J. Non-Cryst. Solids **212**, 157 (1997).
[10]T. Wagner, G. Dale, P. J. S. Ewen, A. E. Owen, and V. Perina, J. Appl. Phys. **87**, 7758 (2000).
[11]A. Kovalskiy, A. C. Miller, H. Jain, and M. Mitkova, J. Am. Ceram. Soc. **91**, 760 (2008).
[12]Y. Sakaguchi, H. Asaoka, Y. Uozumi, Y. Kawakita, T. Ito, M. Kubota, D. Yamazaki, K. Soyama, M. Ailavajhala, M. R. Latif, and M. Mitkova, Can. J. Phys. **92**, 654 (2014).
[13]Y. Sakaguchi, H. Asaoka, Y. Uozumi, Y. Kawakita, T. Ito, M. Kubota, D. Yamazaki, K. Soyama, M. Ailavajhala, M. R. Latif, K. Wolf, M. Mitkova, and W. A. Skoda, J. Phys. Conf. Ser. **619**, 012046 (2015).
[14]Y. Sakaguchi, H. Asaoka, Y. Uozumi, Y. Kawakita, T. Ito, M. Kubota, D. Yamazaki, K. Soyama, M. Ailavajhala, K. Wolf, M. Mitkova, and M. W. A. Skoda, JPS Conf. Proc. **8**, 031023 (2015).
[15]Y. Sakaguchi, H. Asaoka, Y. Uozumi, Y. Kawakita, T. Ito, M. Kubota, D. Yamazaki, K. Soyama, G. Sheoran, and M. Mitkova, Phys. Status Solidi A **213**(7), 1894–1903 (2016).
[16]O. S. Heavens, *Optical Properties of Thin Solid Films* (Butterworth, London, 1955).
[17]*X-ray and Neutron Reflectivity: Principles and Applications*, Lecture Notes Physics 770, edited by J. Daillant and A. Gibaud (Springer, Berlin, Heidelberg, 2009).
[18]J. Als-Nielsen and D. McMorrow, *Elements of Modern X-ray Physics*, 2nd ed. (Wiley, 2011).
[19]D. S. Silvia, *Elementary Scattering Theory for X-ray and Neutron Users* (Oxford University Press, Oxford, 2011).
[20]F. Brido, J. Gautier, F. Delmotte, M.-F. Ravet, O. Durand, and M. Modreanu, Appl. Surf. Sci. **253**, 12 (2006).
[21]K. Sakurai, M. Mizusawa, and M. Ishii, Trans. Mater. Res. Soc. Jpn. **33**, 523 (2008).
[22]M. Takeda, D. Yamazaki, K. Soyama, R. Maruyama, H. Hayashida, H. Asaoka, T. Yamazaki, M. Kubota, K. Aizawa, M. Arai, Y. Inamura, T. Itoh, K. Kaneko, T. Nakamura, T. Nakatani, K. Oikawa, T. Ohhara, Y. Sakaguchi, K. Sakasai, T. Shinohara, J. Suzuki, K. Suzuya, I. Tamura, K. Toh, H. Yamagishi, N. Yoshida, and T. Hirano, Chin. J. Phys. **50**, 161 (2012).
[23]A. Nelson, J. Appl. Crystallogr. **39**, 273 (2006).
[24]P. B. Johnson and R. W. Christy, Phys. Rev. B **6**, 4370 (1972).
[25]R. K. Pan, H. Z. Tao, H. C. Zang, C. G. Lin, T. J. Zhang, and X. J. Zhao, J. Non-Cryst. Solids **357**, 2358 (2011).
[26]T. Kawaguchi, S. Maruno, and K. Tanaka, J. Appl. Phys. **73**, 4560 (1993).
[27]G. Kluge, Phys. Status Solidi A **101**, 105 (1987).
[28]K. Tanaka, J. Non-Cryst. Solids **137–138**, 1021 (1991).
[29]S. R. Elliott, J. Non-Cryst. Solids **130**, 85 (1991).
[30]M. Aniya, J. Non-Cryst. Solids **198–200**, 762 (1996).
[31]T. Kawaguchi and S. Maruno, J. Appl. Phys. **71**, 2195 (1992).
[32]T. Wagner, M. Frumar, and V. Suskova, J. Non-Cryst. Solids **128**, 197 (1991).
[33]D. Goldschmidt and P. S. Rudman, J. Non-Cryst. Solids **22**, 229 (1976).
[34]T. Kawaguchi, S. Maruno, and S. R. Elliott, J. Appl. Phys. **79**, 9096 (1996).
[35]P. G. de Gennes, F. Brochard-Wyart, and D. Quere, *Capillarity and Wetting Phenomena: Drops, Bubbles, Pearls, Waves*, translated by A. Reisinger (Springer-Verlag Inc., New York, 2004).
[36]H. Hisakuni and K. Tanaka, Science **270**, 974 (1995).
[37]A. Mishchenko, J. Berashevich, K. Wolf, D. A. Tenne, A. Reznik, and M. Mitkova, Opt. Mater. Express **5**, 295 (2015).
[38]M. Aniya and T. Shinkawa, J. Mater. Sci.: Mater. Electron. **18**(Suppl. 1), 247–250 (2007).
[39]M. David, R. Padiyath, and S. V. Babu, AIChE J. **37**, 367 (1991).
[40]J. Seth, R. Padiyath, and S. V. Babu, J. Vac. Sci. Technol. A **10**, 284 (1992).
[41]M. Takahashi, T. Maeda, K. Uemura, J. Yao, Y. Tokuda, T. Yoko, H. Kaji, A. Marcelli, and P. Innocenzi, Adv. Mater. **19**, 4343 (2007).
[42]Y. Sakaguchi and K. Tamura, J. Non-Cryst. Solids **205–207**, 115 (1996).
[43]Y. Sakaguchi and K. Tamura, J. Phys.: Condens. Matter **7**, 4787 (1995).